PB86-156957

Study of Rapping Reentrainment Emissions from a Pilot-Scale Electrostatic Precipitator

Southern Research Inst., Birmingham, AL

Prepared for

Environmental Protection Agency
Research Triangle Park, NC

1984

U.S. Department of Commerce
National Technical Information Service
NTIS

TECHNICAL REPORT DATA
(Please read Instructions on the reverse before completing)

1. REPORT NO. EPA/600/J-84/356	2.
3. PB86-156957	
4. TITLE AND SUBTITLE: Study of Rapping Reentrainment Emissions from a Pilot-scale Electrostatic Precipitator (Journal Version)	5. REPORT DATE: 1984
	6. PERFORMING ORGANIZATION CODE
7. AUTHOR(S): P. Vann Bush	8. PERFORMING ORGANIZATION REPORT NO.
9. PERFORMING ORGANIZATION NAME AND ADDRESS: Southern Research Institute, 2000 Ninth Avenue, South, Birmingham, Alabama 35255-5305	10. PROGRAM ELEMENT NO.
	11. CONTRACT/GRANT NO. CR-808973-01
12. SPONSORING AGENCY NAME AND ADDRESS: EPA, Office of Research and Development, Air and Energy Engineering Research Laboratory, Research Triangle Park, NC 27711	13. TYPE OF REPORT AND PERIOD COVERED: Journal Article; 10/83-3/84
	14. SPONSORING AGENCY CODE: EPA/600/13

15. SUPPLEMENTARY NOTES: AEERL project officer is Leslie E. Sparks, Mail Drop 61, 919/541-2458. Published in Environ. Sci. Technol., Vol. 18, No. 9 (Sep. 1984), pp. 699-705.

16. ABSTRACT: The article gives results of a test program to determine the quantity and size distribution of rapping reentrainment emissions from a large pilot-scale electrostatic precipitator (ESP) at TVA's Bull Run steam plant. The ESP current density and specific collection area were varied during the testing. The data were compared to information from full-scale ESPs that had been used to derive generic relationships for rapping reentrainment incorporated in the mathematical model of precipitation. The studies showed that the character of the rapping emissions measured on the pilot ESP differs from the generic rapping used in the ESP model.

17. KEY WORDS AND DOCUMENT ANALYSIS

a. DESCRIPTORS	b. IDENTIFIERS/OPEN ENDED TERMS	c. COSATI Field/Group
Pollution	Pollution Control	13B
Electrostatic Precipitators	Stationary Sources	13I
Emission	Rapping Reentrainment	14G
Dust		11G

18. DISTRIBUTION STATEMENT: Release to Public	19. SECURITY CLASS (This Report): Unclassified	21. NO. OF PAGES: 8
	20. SECURITY CLASS (This page): Unclassified	22. PRICE

EPA Form 2220-1 (9-73)

REPRODUCED BY NATIONAL TECHNICAL INFORMATION SERVICE U.S. DEPARTMENT OF COMMERCE SPRINGFIELD, VA. 22161

Environ. Sci. Technol. 1984, 18, 699–705

EPA/600/J-84/356
JOURNAL ARTICLE

Study of Rapping Reentrainment Emissions from a Pilot-Scale Electrostatic Precipitator

P. Vann Bush

Southern Research Institute, Birmingham, Alabama 35255–5305

■ A test program was conducted to determine the quantity and size distribution of rapping reentrainment emissions from a large pilot scale electrostatic precipitator at the TVA Bull Run Steam Plant. The precipitator current density and specific collection area were varied during the test program. The data were compared to information from full-scale precipitators which had been used to derive generic relationships for rapping reentrainment incorporated in the mathematical model of precipitation.

Introduction

A characterization of the rapping contribution to emissions from a pilot-scale electrostatic precipitator (ESP) was performed in order to evaluate an hypothesis that rapping-related emissions were responsible for the discrepancy between performance measurements and ESP model predictions of performance. The pilot-scale ESP has a gas volume capacity of 30,000 acfm. The internal arrangement of the system is shown in the schematic sectional side view in Figure 1. The precharger field was not energized for this study. The collector stage consists of four standard Lodge–Cottrell design electrical fields of 9-, 6-, 6-, and 9-ft lengths in the direction of gas flow. There are three rapping fields: fields 2 and 3 share 12 ft long collection plates. The total plate height in all fields is 12 ft, with an active height of 10 ft 3 in. There are 13 gas passages in the collector stage, with 10-in. width, giving a total active collection surface of 7995 ft^2. The discharge electrodes installed in the system were $^9/_{16}$-in. diameter wires mounted in the Lodge–Cottrell mast design frame. The pilot scale ESP system has been more thoroughly described in other reports (*1*, *2*).

The ESP model used for predicting the performance of the pilot-scale ESP incorporates a rapping loss calculation based on a limited field study of full-scale electrostatic precipitators (*3*, *4*). The study was conducted at four cold-side ESP installations and two hot-side ESP's. In order to discover a relationship useful in predicting rapping losses, the limited data were plotted as a function of dust calculated to have been removed by the last field of the ESP. The dust removal in the last field was approximated by applying the Deutsch equation in the form

$$\eta/\text{section} = 1 - \exp(-x/N) \qquad (1)$$

where $x = -\ln(1 - \eta_o)$, η_o = overall mass collection fraction determined from mass train measurements, and N = number of ESP sections. These data are plotted in Figure 2. The exponential relationships shown for the hot-side and cold-side ESP data were presented in the rapping study (*4*) as merely aids for interpolation. It was also stated that additional data under a wider variety of conditions were required to verify the validity of this approach. With these caveats the exponential relationships shown in Figure 2 were placed in the model and have been in use since 1978. The relationships are employed in the ESP model to predict the total mass emissions due to rapping. The information generated in this way is all that is used in this model to produce penetration (or collection efficiency) numbers "corrected for rapping reentrainment".

Additional information about the rapping emissions is required to define the fractional penetration (the penetration of particles as a function of their diameter). To provide this information for the model, the data from the limited study were used to compute the apparent rapping puff size distribution at each plant. Figure 3 shows these data. A representative rapping puff size distribution was extracted from the average of the data shown in Figure 3 and approximated by a log-normal size distribution having a mass median diameter (MMD) of 6 μm and a standard deviation of 2.5. When the ESP model has determined the quantity of mass in the rapping emissions using the exponential relationships in Figure 2, the mass is divided into size fractions coinciding with the log-normal distribution.

With the limitations in the data base from which the ESP model treatment of rapping reentrainment was derived, and the differences which may exist between full-scale and large pilot-scale operation, it is reasonable to expect the model is not accurately predicting the contribution of rapping reentrainment to the emission of the pilot ESP.

Test Program

Tests were designed to quantify the percentage of emissions due to rapping in the pilot ESP. The measurements selected to gather this information were method

0013-936X/84/0918-0699$01.50/0 © 1984 American Chemical Society

NTIS is authorized to reproduce and sell this report. Permission for further reproduction must be obtained from the copyright owner.

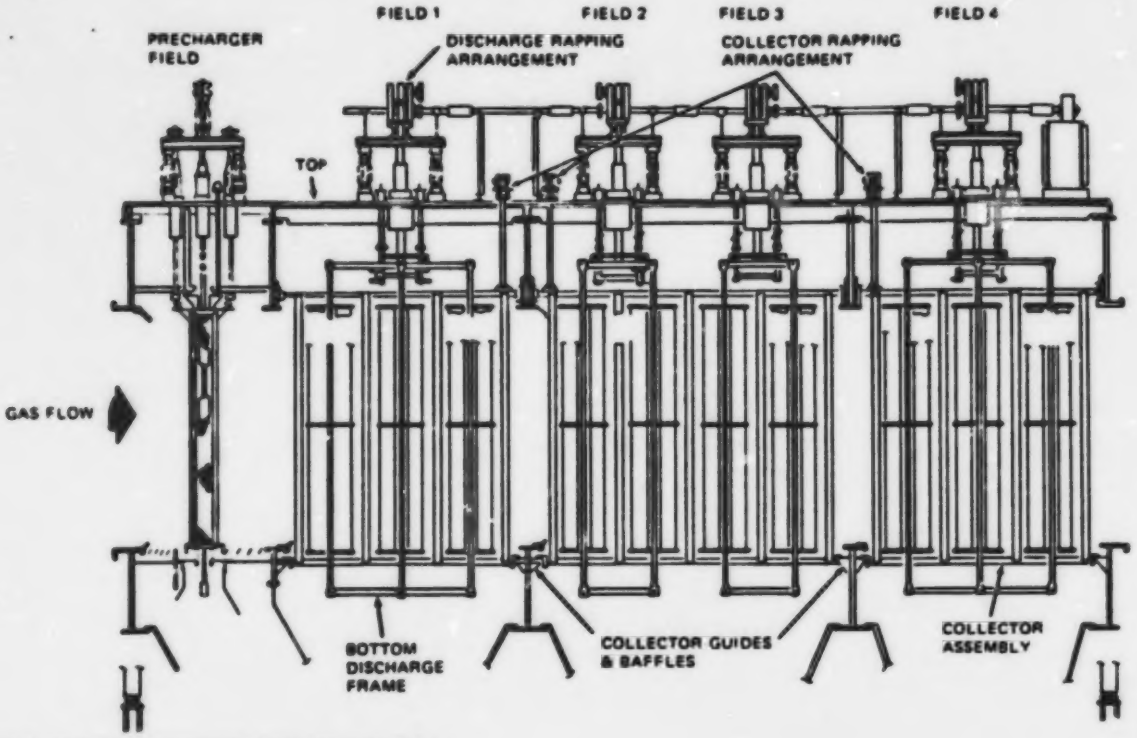

Figure 1. Internal arrangement of the pilot scale ESP.

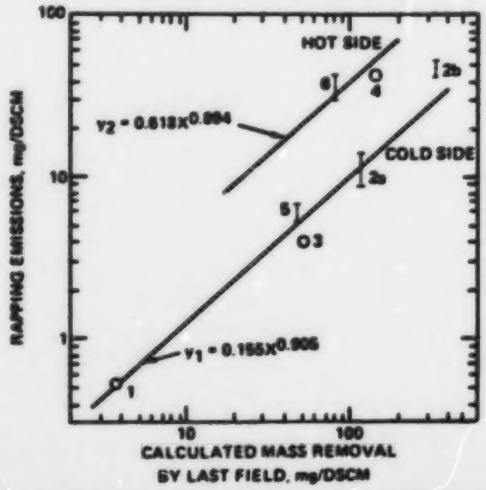

Figure 2. Relationship used in the ESP model to describe rapping emissions as a function of dust removal by the last field.

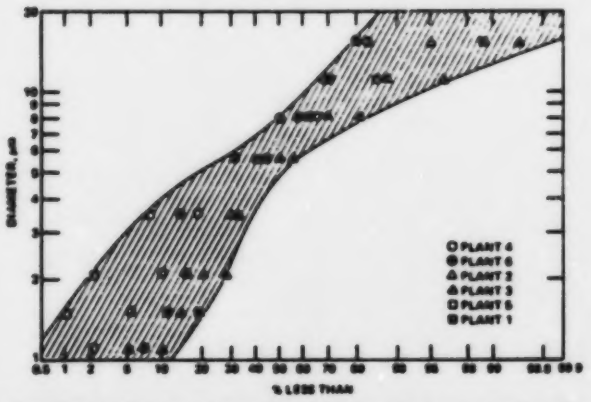

Figure 3. Apparent rapping puff size distribution data used to derive a generic rapping puff for the ESP model.

17 mass loadings (5), cascade impactor fractional mass loadings, and optical measurements of particulate concentrations in real time for large particle sizes. The method 17 measurements were made at the inlet and outlet of the ESP. The outlet measurements were made during either no-rap or rap intervals. From these measurements the percentage of total mass emissions due to rapping could be determined.

Cascade impactor measurements using University of Washington Mark V impactors were also made at the inlet and outlet of the pilot ESP. Measurements at the outlet were made during either no-rap or rap intervals. These data permit the calculation of the size distribution of the rapping puff and the fractional penetration during both base-line and rapping periods.

The large particle sampling system (LPSS), which provides real-time measurements of relative particulate concentrations (4), was installed at the outlet of the pilot ESP. The LPSS data are also useful in determining the amount of fractional penetration due to rapping. The principal advantage of the LPSS over impactors is the continuous monitoring ability which provides information that is irretrievably imbedded in integrated sample data.

Conditions Tested. The pilot ESP was fitted with $^3/_8$-in. diameter discharge wires at the time of this test. The rapping cycles in the sections were 6 raps/h in section 1, 2 raps/h in sections 2 and 3 (rapped concurrently due to the collector sectionalization), and 1 rap/$3^1/_2$ h in section 4. The cycle in section 4 had been adjusted to this frequency in previous attempts to minimize the rapping contribution to emissions. The rapping cycle was not varied during the test.

The key variable in the test program was the average current density. Essentially two current density levels were

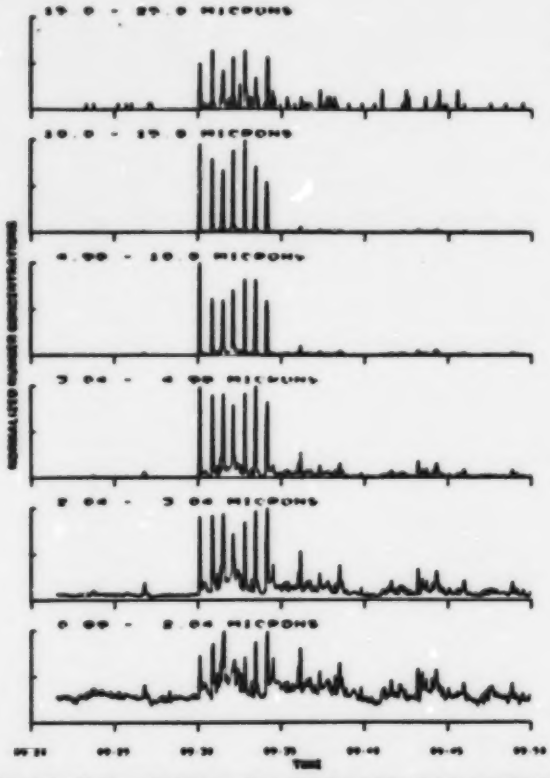

Figure 4. Outlet emissions vs. time showing peaks due to rapping the outlet field.

tested. This was accomplished by operating the pilot ESP at the lowest stable operating condition with the four electrical sections energized independently and then energized with two sections connected to one transformer/rectifier set and controller. This energization scheme yielded average current densities from 5.9 to 2.7 $\mu A/ft^2$. The electric field strength varied from 3.8 to 3.3 kV/cm.

The specific collection area (SCA) in the pilot ESP was also varied by deenergizing section 2, holding the flue gas parameters fixed. This reduced the SCA from 287 to 222 ft^2/kacfm (square feet per 1000 actual cubic feet per minute). The average current density in the low SCA test was 3.5 $\mu A/ft^2$. Only 2 days of testing were conducted at the reduced SCA. There were 4 days of tests at the normal SCA of 287 ft^2/kacfm.

Method Used To Isolate Rapping Emissions. The normal mode of operation for the plate rapper system is to distribute the rapping of the plates in a section over the duration of the rapping cycle. The pilot ESP collector has 14 plates per section (13 gas passages). The collection plates are connected together in pairs, so that seven separate raps are included in the rapping of a section. Normally these separate raps occur sequentially at 30-min intervals in the last section, resulting in a period of $3^1/_2$ h between raps on a given pair of collection plates. In order to facilitate the sampling and improve the satistics for the rapping reentrainment emissions, the rapping in the last field was altered. The 30-min interval between raps was eliminated, and the seven pairs of plates were rapped in rapid succession. The $3^1/_2$-h interval between raps on a given plate was maintained. This method produced an emission profile such as is shown in Figure 4. These data were acquired by the LPSS.

"No-rap" sampling intervals for both impactor and method 17 measurements were those periods preceding the rapping of the fourth section. "Rap" samples with impactors and method 17 samplers were taken during the entire period while rappers were on and typically included no more than 30 min of sample time after the last rap.

The procedure used to interpret the data taken in this manner and to calculate the fraction of emissions attributable to rapping reentrainment was a weighted time average of the rap emissions vs. the no-rap or base-line emissions, each normalized to the $3^1/_2$-h cycle time of the rappers in the fourth field.

The cascade impactor data were deciphered by using the computer program Cascade Impactor Data Reduction System (CIDRS) (6). Impactor runs were identified as inlet, rapping, or base line; all the runs in each category that were made at the same test condition were combined to produce average inlet, rapping, and base-line data sets. Particle size distributions were constructed for each case. The differential size distributions, in terms of $dM/d \log D$, were given for the rapping and base-line emissions. The comparison of the $dM/d \log D$ distributions reveals the amount of mass emission as a function of particle diameter which is due to rapping.

Test Results. (1) Method 17. The outlet mass loadings calculated from method 17 samples are recorded in Table I. The average value of current density which was recorded by a computer data acquisition system (*1*) during each measurement is given in the table. Despite the scattering in the sample population, a trend is indicated which would agree with expected behavior: mass emissions diminish as the current density increases.

The percentage of the emission due to rapping was calculated from time-weighted averages, as shown in the table. The data show an average value of 43.6% of the emissions was due to rapping reentrainment when the precipitator SCA was 287 ft^2/kacfm. This percentage did not show a dependence on current density. The base-line collection efficiency at this SCA averaged 99.75%. The weighted efficiency including rapping emissions averaged 99.57%.

A large difference in rapping emissions was observed between the two values of SCA which were tested. With an SCA of 222 ft^2/kacfm the emissions due to rapping averaged 15.1% of the total emissions. The average base-line collection efficiency at this SCA was measured to be 99.08%, and the weighted efficiency including rapping emissions averaged 98.93%.

Method 17 results have been compared to the ESP model predictions on the basis of the relationship presented in Figure 2. The model basis for determining rapping emissions yields values for mass loadings attributable to rapping which are 2–3 times less than measured emissions. The measured values lie within the region bounded by the model relationships for hot-side and cold-side ESP's. The ESP model would predict 28.7% of emissions due to rapping at the SCA of 287 ft^2/kacfm, whereas the measured value was 43.6%.

(2) Impactors. The data taken with cascade impactors were divided into three groups corresponding to three distinct operating conditions. Measurements made during other conditions were excluded from the analysis. The three conditions are (a) 4.7 $\mu A/ft^2$ current density with an SCA of 287 ft^2/kacfm, (b) 2.8 $\mu A/ft^2$ current density with an SCA of 287 ft^2/kacfm, and (c) 3.5 $\mu A/ft^2$ current density with an SCA of 222 ft^2/kacfm. It should be pointed out that the data shown in the figures include those points on the curves which CIDRS fits to the measured data (6).

The particle size distributions measured during the condition with 4.7 $\mu A/ft^2$ current density and 287 ft^2/

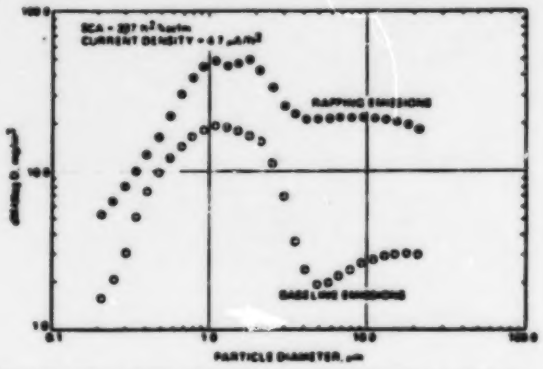

Figure 5. Mass distribution of rapping and base-line emissions.

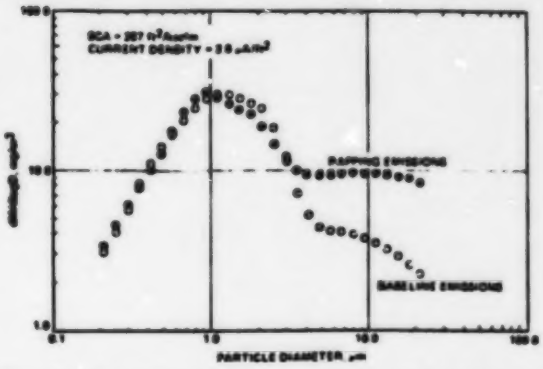

Figure 7. Mass distribution of rapping and base-line emissions.

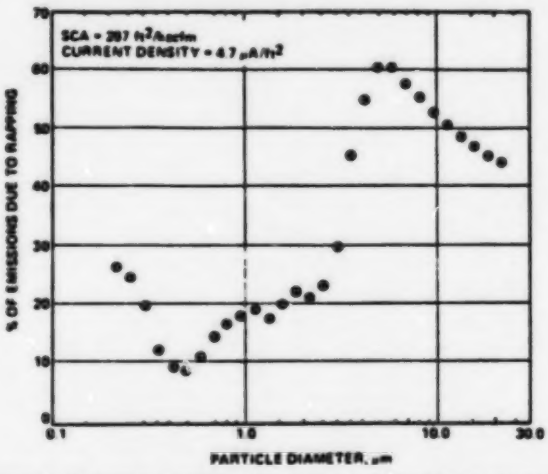

Figure 6. Percent of emissions due to rapping derived from cascade impactor data.

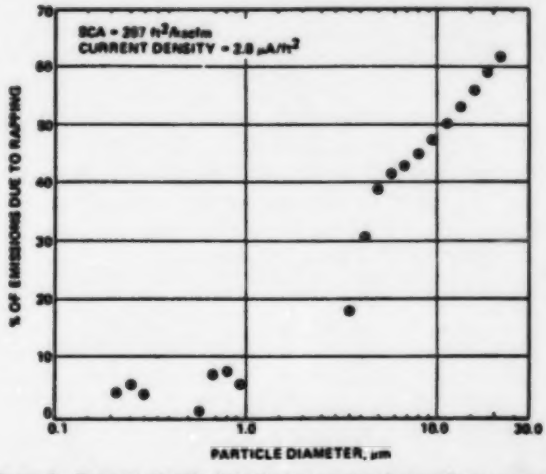

Figure 8. Percent of emissions due to rapping derived from cascade impactor data.

kacfm SCA indicate that at this condition a contribution to the emissions in the form of a rapping puff occurs for all particle sizes measured by the impactor. This result is evident in the plot of dM/d log D given in Figure 5. A percent of emissions due to rapping was determined as a function of particle size from the mass distributions presented in Figure 5 and is simply the difference between the base-line and rapping emissions. This result is given in Figure 6 (The uncertainty in the data is not presented in the figures but could account for the apparent decrease in the rapping contribution to emissions for particle diameters > 7 μm.)

The results of the impactor measurements made at 2.8 μA/ft² current density and 287 ft²/kacfm SCA indicate that in this case there is little difference evident in particle size distributions for base-line and rapping periods except for the particle diameters greater than ~1 μm. In fact, the plot of dM/d log D vs. particle diameter, which is given in Figure 7, reveals that the rapping emissions are significantly different from the base-line emissions for just those particles with diameters greater than ~2 μm. This result, when translated to the form of percent of emissions due to rapping, is presented in Figure 8.

The results of impactor measurements at the reduced SCA (222 ft²/kacfm) are similar to the low current density case at the larger SCA; the rapping reentrainment significantly contributes to the emissions beginning with particles of ~2-μm diameter. The percent of emissions is much lower in this case than either of the conditions with the larger SCA, which is in accord with method 17 data.

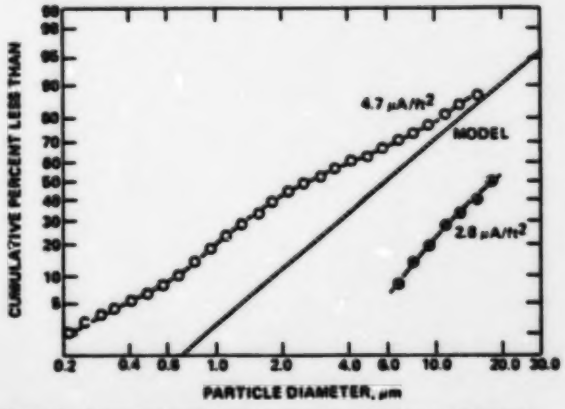

Figure 9. Measured and generic rapping puff size distributions.

In order to calculate the size distribution of the rapping puffs for the two conditions at 287 ft²/kacfm, the cumulative mass concentrations and the calculated mass loadings were analyzed. The cumulative mass concentration in the rapping puff is equal to the cumulative mass concentration measured during the rapping period minus the cumulative mass concentration measured during the base-line period. The amount of total mass in the rapping puff is the difference between the calculated mass loadings for the rapping and base-line samples. From these calculations the rapping puff size distributions presented in Figure 9 were derived. The size distribution used in the ESP model is also shown in Figure 9.

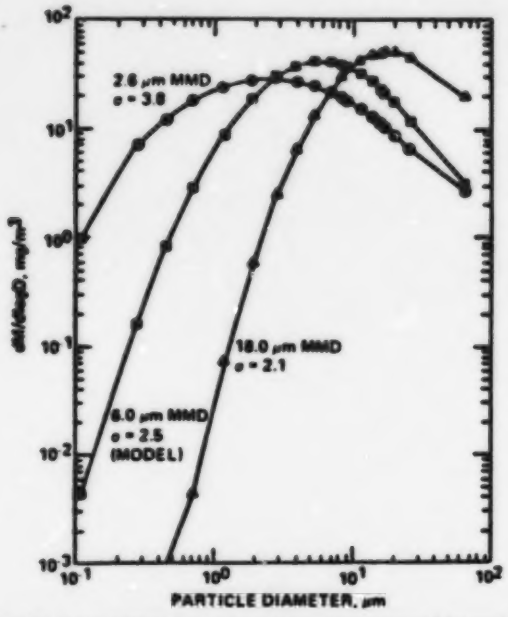

Figure 10. Mass distribution of three different rapping puffs normalized to a given total mass.

By use of the relationships for log-normal distribution given

$$\sigma \simeq \frac{D_{50}}{D_{16}} \tag{2}$$

or

$$\sigma \simeq \left(\frac{D_{84}}{D_{16}}\right)^{1/2} \tag{3}$$

the calculated rapping puff size distributions can be defined by their MMD, or D_{50}, and standard deviation σ. For the condition with a current density of 4.7 $\mu A/ft^2$ the rapping puff has an MMD of 2.6 μm and σ of 3.8. For the condition with a current density of 2.8 $\mu A/ft^2$ the rapping puff has an MMD of 18.0 μm and σ of 2.1. This indicates a relationship exists between the rapping puff size distribution and the ESP current density. The distributions of the mass in the rapping puffs are shown in Figure 10. Shown in this figure are the two calculated rapping puffs and the rapping puff used in the ESP model. The rapping puffs are normalized to a given total mass loading. The ESP model was run with two of the rapping puffs to determine what effect the difference would have on calculated emissions. The difference in the character of the emissions, as shown in plots of $dM/d \log D$ vs. particle size, becomes significant at particle diameters greater than ~8 μm in this case.

(3) Large Particle Sampling System. The primary use of data acquired with the LPSS was to monitor real-time variations in outlet emissions and relate those variations to rapping reentrainment. Figure 4 is illustrative of the ability of the LPSS to monitor the transient emissions caused by rapping. These data were taken when the ESP was operated at a current density of 5.1 $\mu A/ft^2$. The rapping puffs are an increasingly dominant fraction of the total emissions at larger particle diameters. The background concentration of particles is greater after the rapping episode which indicates that some instability in the collected dust layer persists for 30 min or longer after rapping. The structure between rapping peaks is evidence of hopper "boil up" of the fallen dust layer. A fast Fourier transform (FFT) of these data reveals the primary frequency associated with the rapping peaks (~90 raps/h) and the related harmonics. This is shown in Figure 11. There is no evidence of any other periodic behavior in the emissions.

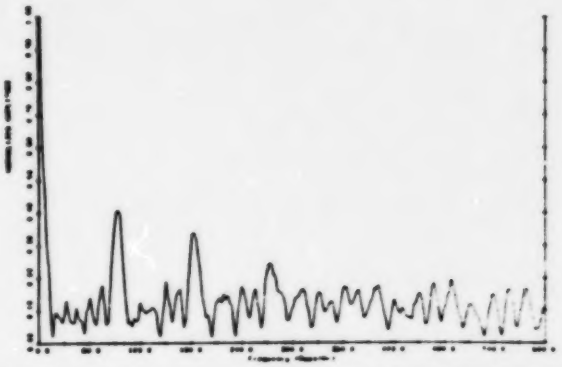

Figure 11. FFT analysis of emissions showing the rapping frequency in the last field.

LPSS data taken when the ESP current density was 2.8 $\mu A/ft^2$ indicate the background level after the rapping period is more noisy than the level shown in the higher current density condition in Figure 4. Another difference was noted in the relative amplitude of rapping and baseline particle concentrations for the smaller particles. The rapping peaks were a more significant perturbation to the particle concentration in these ranges for the higher current density case. This result is in qualitative agreement with the impactor data. The rapping emissions at 2.8 $\mu A/ft^2$ current density are also accompanied with hopper boil-up emissions. FFT analysis of the data at this current density duplicates results found in the case of higher current density.

In order to try to isolate effects of upstream rappers in the outlet emissions, the last field of the pilot ESP was turned off while sections 2 and 3 were rapped. These LPSS data again revealed the primary and harmonic frequencies associated with the raps in the FFT output. Section 4 was then energized, and the LPSS acquired data while sections 2 and 3 were rapped. These data were analyzed by using FFT. The collection of the last field of the ESP removes the upstream rapping puffs. They are no longer discernible in the emissions.

Conclusions

The character of the rapping emissions measured on the pilot ESP differs from the generic rapping used in the ESP model. The fraction of total mass emissions attributable to rapping reentrainment measured to be higher than the model predicts by as much as a factor of 2 or 3. The measured values lie between the relationships that the model uses for hot-side and cold-side ESP rapping emissions and are not far outside the scatter of the data used to derive those relationships. The discrepancy between measured and predicted performance for the pilot ESP, which instigated this study, cannot be resolved by adjusting the percent of emissions due to rapping used in the model. Use of the measured values causes greater variance between performance predictions and performance measurements. The model is unable to accurately predict the base-line, or no-rap, efficiency of the pilot ESP as it was configured for this test.

The rapping puff size distribution was found to depend on current density. This relationship is not included in the ESP model. The model uses a generic rapping puff

Table I. Outlet Method 17 measurements results.

DATE	FLUE TEMP (°F)	SCA (ft^2/Kacfm)	SAMPLE TIME (min)	AVERAGE COLLECTOR CURRENT DENSITY ($\mu A/ft^2$)	BASELINE OR RAPPING SAMPLE	MASS LOADING (gr/scf)	COLLECTION EFFICIENCY (%)	AVERAGE DAILY BASELINE LOADING (gr/scf)	LOADING DUE TO RAPS (gr/scf)	RAPPING EMISSION NORMALIZED TO 3½ HR CYCLE (gr/scf)	RAP + BASELINE EMISSIONS (gr/scf)	% EMISSIONS DUE TO RAPS
3/18	311	222	7	5.20	Rapping	0.202	99.37	0.0289	0.173	0.00577	0.0347	16.6
	310		40	5.00	Baseline	0.0247						
	314		10	5.15	Rapping	0.151			0.122	0.00583	0.0347	16.8
	315		40	3.14	Baseline	0.0331						
3/19	310		10	3.90	Rapping	0.196	99.16		0.153	0.00729	0.0504	14.5
	311		40	3.62	Baseline	0.0382	99.03	0.0431				
	311		10	3.34	Rapping	0.185			0.142	0.00677	0.0499	13.6
	314		40	3.30	Baseline	0.0480	98.78					
3/20	313	267	30	4.57	Rapping	0.0671	99.71	0.00973	0.0574	0.00819	0.0179	45.7
	315		60	4.68	Baseline	0.0116						
	317		30	4.83	Rapping	0.0555			0.0458	0.00654	0.0163	40.2
	317		60	3.96	Baseline	0.00786	99.80					
	315		30	4.53	Rapping	0.0478			0.0380	0.00543	0.0152	35.8
3/21	315		30	3.59	Rapping	0.0954		0.0140	0.0815	0.0116	0.0256	45.5
	314		60	2.90	Baseline	0.0126	99.68					
	312		30	2.75	Rapping	0.0855			0.0716	0.0102	0.0242	42.3
	318		60	2.68	Baseline	0.0154	99.61					
	314		30	2.83	Rapping	0.0873			0.0734	0.0105	0.0244	42.9
3/22	313		30	5.50	Rapping	0.0637		0.00685	0.0559	0.00798	0.0158	50.4
	313		70	5.90	Baseline	0.00829	99.79					
	316		30	4.00	Rapping	0.0547			0.0468	0.00669	0.0145	46.0
	317		60	4.10	Baseline	0.00741	99.81					
	319		30	3.90	Rapping	0.0533			0.0456	0.00650	0.0143	45.3
3/23	315		30	5.12	Rapping	0.0330		0.00568	0.0274	0.00391	0.00958	40.8
	315		240	4.79	Baseline	0.00568	99.86					
	322		30	5.30	Rapping	0.0382			0.0325	0.00465	0.0103	45.0

[a] Computed using average inlet loading for all test days (3.95 gr/scf)

size distribution which has an MMD which lies between the values measured at two test conditions. In the absence of a large base of data the generic rapping puff is a reasonable approximation for predicting performance from uncharacterized sources.

The LPSS data show qualitative agreement with method 17 and impactor measurement results. The LPSS data indicate that a relatively small fraction of the rapping reentrainment is due to hopper boil up. There is evidence that rapping episodes are followed by periods of dust layer instability in which emissions decline. Also resolved from these data is the fact that rapping reentrainment only from the last field can be isolated in the emissions. Although these results cannot be generalized without corroboration

from other tests, they were consistent over the range of conditions tested in this study.

Acknowledgments

The efforts of Todd Snyder, Wallace Kistler, Bob Hammond, Steve Hall, and Terry Hammond in executing the test program are gratefully acknowledged. The guidance and direction of EPA Project Officer Leslie Sparks are appreciated.

Literature Cited

(1) Bush, P. V.; Pontius, D. H. In "Third Symposium on the Transfer and Utilization of Particulate Control Technology: Control of Emissions from Coal Fired Boilers"; U.S. Environmental Protection Agency: Washington, DC, July 1982; Vol. I, EPA-600/9-82-005a.

(2) Bush, P. V.; Pontius, D. H., presented at the Fourth Symposium on the Transfer and Utilization of Particulate Control Technology, Houston, TX, Oct 1982.

(3) Mosley, R. B.; Anderson, M. H.; McDonald, J. R. "A Mathematical Model of Electrostatic Precipitation". Feb 1980, EPA-600/7-80-034 (NTIS PB80-190994) (Revision 2).

(4) Gooch, J. P.; Marchant, G. H., Jr. Palo Alto, CA, Aug 1978, EPRI Report RP-792, Vol. 3.

(5) *Fed. Reg.* 1976, *41*, 187, 42020.

(6) Johnson, J. W.; Clinard, G. I.; Felix, L. G.; McCain, J. D. "A Computer-Based Cascade Impactor Data Reduction System". EPA-600/7-78-042 (NTIS PB-285433).

Received for review October 13, 1983. Accepted March 29, 1984. This work was funded under EPA Cooperative Agreement CR-808973-01.

NOTICE

This document has been reviewed in accordance with U.S. Environmental Protection Agency policy and approved for publication. Mention of trade names or commercial products does not constitute endorsement or recommendation for use.

This article documents research that was conducted under the auspices of the U.S. Environmental Protection Agency (USEPA). As an arm of the government, the USEPA has a paid up, non-exclusive, irrevocable, worldwide license to reproduce, prepare derivative works, and distribute to the public all of the material contained herein, and to grant others acting on its behalf the right to do so. The USEPA grants to the National Technical Information Service, Department of Commerce, the right to act as its agent in the distribution of this material.